



## LETTERS TO THE EDITOR



### LARGE-AMPLITUDE LIMIT CYCLES VIA A HOMOCLINIC BIFURCATION MECHANISM

ANUPAM SHARMA<sup>†</sup> AND N. ANANTHKRISHNAN

*Department of Aerospace Engineering, Indian Institute of Technology, Bombay, Powai, Mumbai 400076,  
India. E-mail: [akn@aero.iitb.ernet.in](mailto:akn@aero.iitb.ernet.in)*

(Received 14 July 1999, and in final form 1 February 2000)

#### 1. INTRODUCTION

Unforced or self-excited periodic oscillations in non-linear dynamical systems are called limit cycles. Limit cycles usually arise at a Hopf bifurcation in non-linear systems with a varying parameter. In mechanical systems, the varying parameter is frequently a damping coefficient. Examples of limit cycles in mechanical systems are flutter of aircraft wings, surge oscillations in axial flow compressors, and wing rock in aircraft flight dynamics.

Regular or normal limit cycles were distinguished from large-amplitude limit cycles by Ananthkrishnan and Sudhakar [1]. Stable normal limit cycles are created at a supercritical Hopf bifurcation with the limit cycle amplitude building up gradually from nought as the parameter is varied from the Hopf bifurcation point. In contrast, stable large-amplitude limit cycles are either created with a finite amplitude or show a sudden increase in amplitude after originating as a normal limit cycle at a Hopf bifurcation point.

Stable large-amplitude limit cycles were characterized in terms of secondary bifurcations by Ananthkrishnan *et al.* [2]. The phenomena of finite amplitude onset, and jump in amplitude were described in terms of secondary fold bifurcations. The presence of large-amplitude limit cycles was seen to be accompanied by hysteresis in the system response with varying parameter. Reference [2] also constructed low order models based on a non-linear damping mechanism that reproduced the essential dynamics associated with the primary Hopf-secondary fold bifurcation pairs characterizing large-amplitude limit cycles. These models were found to provide a suitable representation of the large-amplitude surge limit cycles in axial flow compressors. However, the models in reference [2] based on a non-linear damping mechanism could not explain the large-amplitude wing rock limit cycles that had been characterized in terms of the same primary Hopf-secondary fold bifurcation pair [1]. Ananthkrishnan *et al.* [3], therefore, came up with another model based on an alternate mechanism involving a pair of resonantly coupled oscillators.

The models in references [2, 3] represented large-amplitude limit cycles created at secondary fold bifurcations following a primary Hopf bifurcation. However, there could be mechanical systems where large-amplitude limit cycles are characterized by a different combination of bifurcations. One such problem arises in the passage through resonance of

<sup>†</sup> Currently at the Department of Aerospace Engineering, Pennsylvania State University, University Park, PA 16802, U.S.A.

rolling finned projectiles with an offset center of mass [4]. The dynamics of these projectiles shows the phenomenon of lock-in at resonance [5, 6]. In some instances, the locked in projectile experiences large-amplitude yawing motion called catastrophic yaw. Catastrophic yaw has been conjectured to be a large-amplitude limit cycling motion, but one that is not characterized by the secondary fold bifurcation mechanism [7].

This, therefore, provides the motivation to seek a model based on an alternate bifurcation mechanism for the creation of large-amplitude limit cycles in mechanical systems. However, application of this model to the catastrophic yaw problem, attempted by Sharma [8], is not within the scope of this Letter.

## 2. MODEL

As in references [2, 3], the supercritical van der Pol oscillator serves as a starting point for the model construction procedure,

$$\ddot{x} + (x^2 + \mu)\dot{x} + x = 0. \quad (1)$$

Equation (1) has one equilibrium point at  $x = 0$  that is stable for  $\mu > 0$  and unstable for  $\mu < 0$ . Loss of stability with varying  $\mu$  occurs at a Hopf bifurcation at  $\mu = 0$  resulting in a family of stable limit cycles for  $\mu < 0$ . In order to create the fold bifurcations, references [2, 3], in essence, augmented equation (1) with additional damping terms. In the present work, equation (1) is modified with additional quadratic and cubic stiffness terms, to give the following augmented model:

$$\ddot{x} + (x^2 + \mu)\dot{x} + k_1x + k_2x^2 + k_3x^3 = 0. \quad (2)$$

The signs of the coefficients of the linear and cubic stiffness terms are so chosen that equation (2) shows multiple equilibrium solutions for all values of the damping coefficient  $\mu$ . It is easily seen that the equilibrium points of equation (2) occur at  $x = 0$ ,  $(-k_2 \pm \sqrt{k_2^2 - 4k_1k_3})/2$ .

*Case A* ( $k_2 = 0$ ). This is the non-generic case, discussed by Jackson [9], where the three equilibrium points are located at  $x = 0$ , and  $x = \pm \sqrt{-k_1k_3}$ , symmetrically about  $x = 0$ . For the following analysis, we choose  $k_1 = -4$ ,  $k_2 = 0$ , and  $k_3 = 1$ . Then, the equilibrium at  $x = 0$  is an unstable saddle, while the other two equilibria are stable foci for  $\mu = 0$ . The sequence of bifurcations with decreasing linear damping parameter  $\mu$  is computed with the AUTO continuation algorithm of Doedel *et al.* [10]. The resulting bifurcation diagram is plotted in Figure 1, which also shows the phase portraits corresponding to the values of  $\mu$  labelled a-d.

With  $\mu$  decreasing from zero, the right outset of the saddle connects with the right inset, and the left outset with the left inset, at the value of  $\mu$  labelled b, giving rise to two simultaneous homoclinic bifurcations, also called a gluing bifurcation. Beyond the homoclinic bifurcation, for instance at a value of  $\mu$  labelled c, the saddle connection gives way to create an unstable limit cycle about each of the stable foci, and a large-amplitude stable limit cycle encircling all the three equilibrium points. The unstable limit cycles vanish at simultaneous subcritical Hopf bifurcations, but the stable limit cycle persists for smaller values of  $\mu$ . The limit cycles in this case are symmetric about  $x = 0$  although this may not be apparent from Figure 1 where only peak limit cycle amplitudes have been plotted.

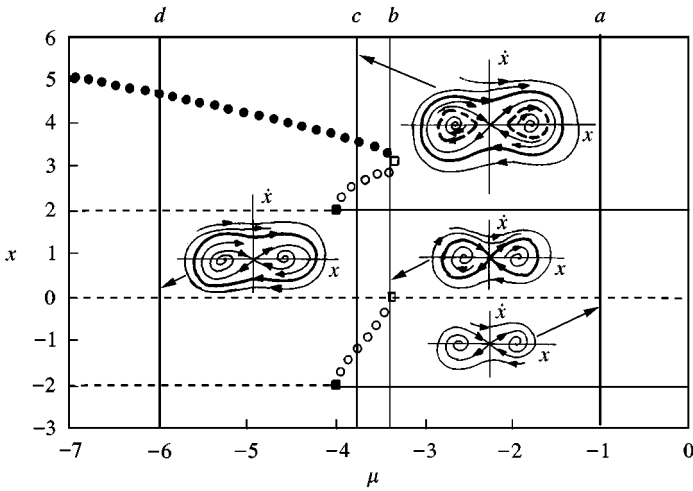


Figure 1. Computed bifurcation diagram for equation (2) with varying linear damping parameter  $\mu$  for the non-generic case of  $k_2 = 0$ . (—: stable equilibria, ---: unstable equilibria, ●—●: stable limit cycle, ○—○: unstable limit cycle, ■—■: Hopf bifurcation, □—□: homoclinic bifurcation). Peak amplitudes of the limit cycle solutions have been depicted. Phase portraits corresponding to values of  $\mu$  labelled *a*, *b*, *c*, *d* are shown as insets.

The birth of the stable large-amplitude limit cycle in Figure 1 is distinct from that at fold bifurcations in references [2, 3]. The saddle loops at the value of  $\mu$  labelled *b* are not limit cycles as they are not periodic. The period tends to infinity as one approaches the homoclinic bifurcation point along either the stable or unstable limit cycle branch. In contrast, at a fold bifurcation, one has a limit cycle with finite period. However, the large-amplitude limit cycles in Figure 1 are similar to those created at a fold bifurcation in that they do show the properties of finite amplitude onset, and hysteresis in the system response with varying parameter. The phenomenon of simultaneous homoclinic bifurcations in Figure 1 is a special case arising due to the equidistance of the stable foci from the saddle point.

*Case B* ( $k_2 \neq 0$ ). This is the generic case where the introduction of the quadratic stiffness term breaks the symmetry in the location of the stable foci about  $x = 0$ . For the following analysis, we choose  $k_1 = -2$ ,  $k_2 = 1$ , and  $k_3 = 1$ . For  $\mu = 0$ , the equilibrium points are an unstable saddle at  $x = 0$ , and a pair of stable foci at  $x = 1$  and  $-2$ . The bifurcation diagram for this case, with  $\mu$  as the parameter, computed by using the AUTO continuation algorithm of Doedel *et al.* [10], is shown in Figure 2. The sequence of bifurcations with decreasing  $\mu$  can be understood with reference to the phase portraits shown in Figure 3. Figure 3(a) shows the phase portrait for  $\mu = 0$ . With decreasing  $\mu$ , the first homoclinic bifurcation occurs when the right outset of the saddle connects with the right inset as shown in Figure 3(b). The homoclinic gives rise to a family of unstable limit cycles about the right focus, shown in Figure 3(c), which terminates at a Hopf bifurcation at  $\mu = -1$ . This leaves the left focus as the only stable solution (Figure 3(d)) until the right outset connects with the left inset in another homoclinic bifurcation, as shown in Figure 3(e). Out of the resulting saddle loop, which encircles both the foci, emerges a family of large-amplitude limit cycles, as shown in Figure 3(f).

With a further decrease in the value of  $\mu$ , the left outset connects with the left inset in yet another homoclinic bifurcation giving rise to a family of unstable limit cycles about the left

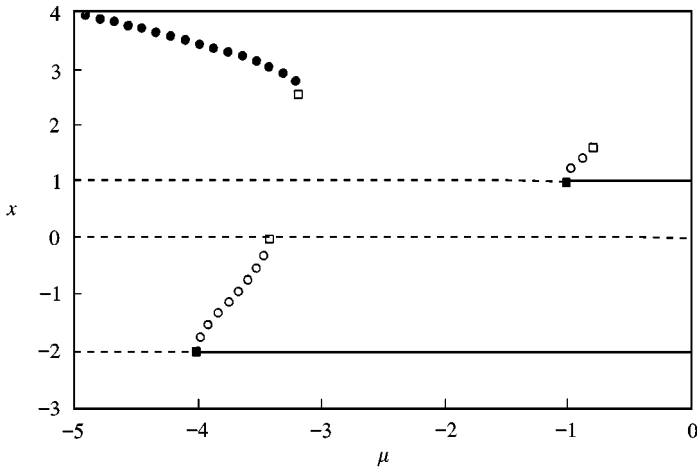


Figure 2. Computed bifurcation diagram for equation (2) with varying linear damping parameter  $\mu$  for the generic case of  $k_2 \neq 0$ . (—: stable equilibria, ---: unstable equilibria, ●—●: stable limit cycle, ○—○: unstable limit cycle, ■—■: Hopf bifurcation, □—□: homoclinic bifurcation). Peak amplitudes of the limit cycle solutions have been depicted.

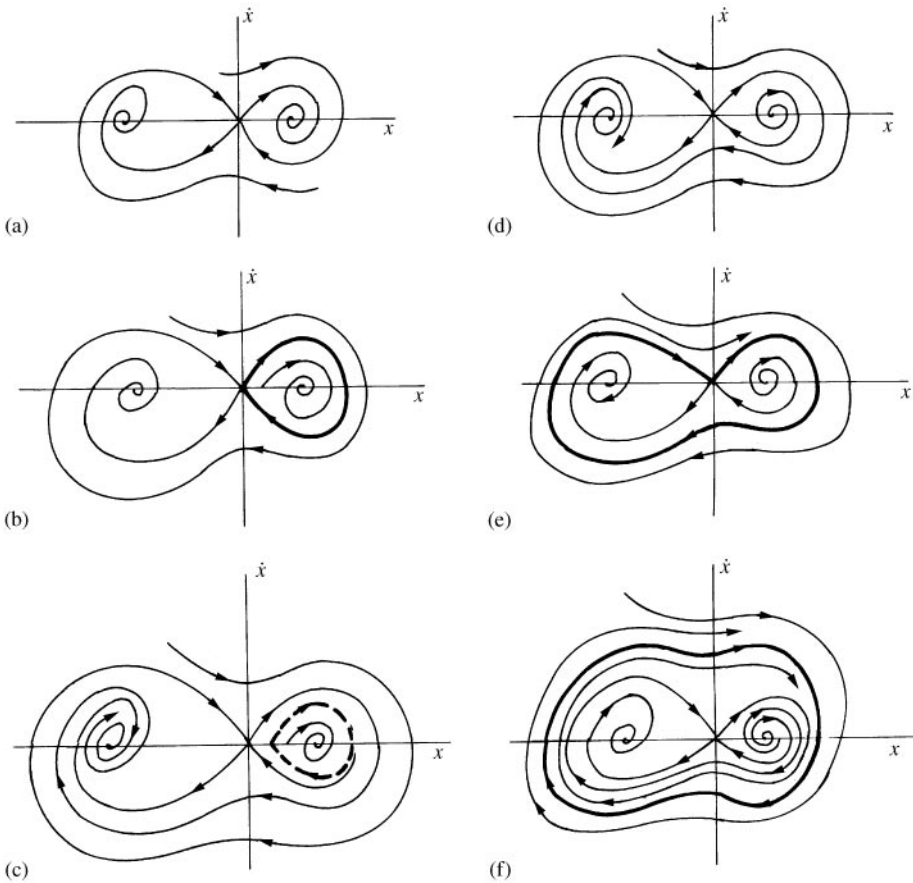


Figure 3. Phase portraits corresponding to the sequence of bifurcations with decreasing values of  $\mu$  in Figure 2. See text for explanation.

focus which end in a subcritical Hopf bifurcation at  $\mu = -4$ . This scenario is identical to that in Figure 3(b-d), and is therefore not sketched separately in Figure 3. The stable large-amplitude limit cycles persist for smaller values of  $\mu$ . Once again, the phenomena of finite amplitude onset, and the hysteresis between the stable large-amplitude limit cycles and the stable left focus with varying parameter, can be noticed.

Computationally, the stable large-amplitude limit cycles in Figure 2 are not a continuation of a limit cycle branch starting or ending at a Hopf bifurcation, and this makes it difficult to locate and track them. Like most continuation algorithms, AUTO does not identify homoclinic bifurcations, and they can be computed only in the limit of a branch of limit cycles as the period goes to infinity. Thus, the computation of the bifurcation diagram in Figure 2 is much more of a challenge than those in references [2, 3] where the limit cycle branch originating at a Hopf bifurcation could be continued past the fold bifurcations to track the large-amplitude limit cycles.

### 3. CONCLUSION

The creation of stable large-amplitude limit cycles in mechanical systems by way of a homoclinic bifurcation mechanism has been described. This provides an alternative to the more common secondary fold bifurcation mechanism analyzed earlier by the authors [2, 3].

### REFERENCES

1. N. ANANTHKRISHNAN and K. SUDHAKAR 1996 *AIAA Journal of Guidance, Control, and Dynamics* **19**, 680–685. Characterization of periodic motions in aircraft lateral dynamics.
2. N. ANANTHKRISHNAN, K. SUDHAKAR, S. SUDERSHAN and A. AGARWAL 1998 *Journal of Sound and Vibration* **215**, 183–188. Application of secondary bifurcations to large-amplitude limit cycles in mechanical systems.
3. N. ANANTHKRISHNAN, S. SUDERSHAN, K. SUDHAKAR and A. VERMA *Journal of Sound and Vibration*. Large-amplitude limit cycles in resonantly coupled oscillators (to appear).
4. A. SHARMA and N. ANANTHKRISHNAN *Journal of Sound and Vibration*. Passage through resonance of rolling finned projectiles with center-of-mass offset (under review).
5. N. ANANTHKRISHNAN and S. C. RAISINGHANI 1994 *Journal of the Institution of Engineers (India)* **74**, 37–43. Theory of resonant lock-in of rolling finned projectiles.
6. N. ANANTHKRISHNAN and S. C. RAISINGHANI 1992 *Journal of Spacecraft and Rockets* **29**, 692–696. Steady and quasisteady resonant lock-in of finned projectiles.
7. N. ANANTHKRISHNAN 1994 *Ph.D. Dissertation, Department of Aerospace Engineering, Indian Institute of Technology, Bombay*. Continuation and bifurcation methods applied to nonlinear problems in flight dynamics.
8. A. SHARMA 1999 *B. Tech. Project Report, Department of Aerospace Engineering, Indian Institute of Technology, Bombay*. Passage through resonance of rolling finned missiles with center-of-mass offset.
9. E. A. JACKSON 1989 *Perspectives of Nonlinear Dynamics*, Vol. 1. Cambridge: Cambridge University Press.
10. E. J. DOEDEL, X. J. WANG and T. F. FAIRGRIEVE 1995 *California Institute of Technology Report*. AUTO94: software for continuation and bifurcation problems in ordinary differential equations.